HZSM-5 and HY Zeolite Catalyst Performance in the Pyrolysis of Tires in a Conical Spouted Bed Reactor

ARTICLE *in* INDUSTRIAL & ENGINEERING CHEMISTRY RESEARCH · OCTOBER 2008

Impact Factor: 2.59 · DOI: 10.1021/ie800376d

6 AUTHORS, INCLUDING:

Miriam Arabiourrutia
Universidad del País Vasco / Euskal Herrik…
18 PUBLICATIONS **321** CITATIONS
SEE PROFILE

Martin Olazar
Universidad del País Vasco / Euskal Herrik…
274 PUBLICATIONS **5,689** CITATIONS
SEE PROFILE

Roberto Aguado
Universidad del País Vasco / Euskal Herrik…
68 PUBLICATIONS **2,000** CITATIONS
SEE PROFILE

Gartzen Lopez
Universidad del País Vasco / Euskal Herrik…
81 PUBLICATIONS **1,454** CITATIONS
SEE PROFILE

HZSM-5 and HY Zeolite Catalyst Performance in the Pyrolysis of Tires in a Conical Spouted Bed Reactor

Miriam Arabiourrutia,[†] Martin Olazar,*[,†] Roberto Aguado,[†] Gartzen López,[†] Astrid Barona,[‡] and Javier Bilbao[†]

Departamento de Ingeniería Química, Universidad del País Vasco, Apartado 644, 48080 Bilbao, Spain, and Departamento de Ingeniería Química y Medio Ambiente, Universidad del País Vasco, Alda. Urquijo s/n, 48013 Bilbao, Spain

A study has been carried out on the in situ use of two catalysts (prepared based on HZSM-5 and HY zeolites) in the pyrolysis of tires in a conical spouted bed reactor at 425 and 500 °C. Both catalysts significantly affect the yields and composition obtained in thermal pyrolysis for the fractions corresponding to C_1-C_4 gases, nonaromatic C_5-C_{10}, aromatic C_{10-}, and tar. The shape selectivity characteristic of each zeolite has a considerable influence on catalyst performance. The HZSM-5 zeolite catalyst produces an increase in the yield of gases, with an increase in the yield of propene and the same yield of butadiene as in thermal pyrolysis, in which it is already high. Concerning the liquid fraction, the catalysts give way to a decrease in the yield of d-limonene (the conical spouted bed reactor performs very well in thermal pyrolysis for this purpose), whereas the yield of BTX aromatics increases, with an increase in the yield of xylenes. A positive fact to be noted is the decrease in the formation of tar (C_{10+}) compared to thermal pyrolysis. As the reaction occurs, a carbonaceous material is deposited on the catalyst, in which the following are identified: (i) carbon black externally coating the particles and deposited on the catalyst macropores and mesopores and (ii) coke deposited on zeolite micropores, due to hydrocarbon condensation activated by catalyst active sites. This condensation preferably takes place in the HY zeolite due to both the larger size of intersections between micropore channels and to greater hydrogen-transfer capacity. Nevertheless, under the reaction conditions tested (up to 10.87 g of tire treated/g of catalyst), product yields remain almost constant, which is evidence that the catalyst does not undergo deactivation.

Introduction

The generation of used tires in 2005 was estimated to be 2.5 million tonnes in North America, 2.5 million in Europe, and 0.5−1.0 million in Japan, which means 6 kg (approximately the weight of a car tire) per inhabitant and year in these developed countries.[1] The forecast for 2012 is that world generation will exceed 17 million tonnes per year, given that economic growth in developing countries drives vehicle sales and the substitution of less deteriorated tires, and the measures adopted to lengthen tire life are insufficient to offset these circumstances.[2] China generated 1 million tonnes in 2005 and the annual increase is 12%. This outlook makes the valorization of used tires more interesting, and among the different technologies, pyrolysis has the following advantages: (i) it enables the subsequent individual valorization of gaseous, liquid, and carbon black fractions, which is an interesting aspect for economic viability;[3] (ii) it has a higher efficiency for energy and a lower environmental impact than incineration.[4]

Different types of reactors have been used for tire pyrolysis, such as autoclaves[5] and fixed bed reactors,[6−10] and for a larger scale operation, bubbling fluidized bed reactors,[9−14] moving beds under vacuum, in one and two steps,[15−17] ablative beds,[18] and rotary ovens.[19−21] Key factors for process viability are high throughput and products with suitable properties for their subsequent valorization toward value added compounds (such as high-quality carbon black, active carbon, or chemical compounds, such as benzene, toluene, xylene, limonene, and so on).

This paper addresses tire pyrolysis in a conical spouted bed reactor, which is of high versatility for gas and solid flow and has suitable features for this process: (i) it allows for handling solids of irregular texture, with a wide particle size distribution, and of sticky nature; (ii) gas−solid heat-transfer rate is high and enhanced by countercurrent flow in the annulus (solid flows downward).[22] Furthermore, it is of simple design, with a lower pressure drop than fluidized beds, and scaling-up is feasible by using several reactors in series or parallel, draft tubes, or multiple spouts.[23,24] This good performance of the conical spouted bed has been proven in catalytic polymerizations,[25,26] in the thermal and catalytic pyrolysis of biomass,[27,28] and in plastic wastes.[29−31] It has also been proven to be suitable for the kinetic study of tire pyrolysis thanks to bed isothermicity and gas flow versatility, given that operation with a short gas residence time allows for minimizing secondary reactions of tire devolatilization products.[32] In a recent paper, a study was carried out on the effect of operating conditions on the yields and composition of tire pyrolysis products.[33]

The aforementioned properties of the conical spouted bed reactor make it suitable for using catalyst particles in situ together with tire particles, without the problems associated with segregation or defluidization by particle agglomeration.[34] In this paper, a study is carried out on the performance of catalysts based on HZSM-5 and HY zeolites with the aim of determining their incidence on the yields of volatile products. Few papers deal with the use of acid catalysts in the pyrolysis of tires, and

* To whom correspondence should be addressed. Phone: 34-94-6012527. Fax: 34-94-6013500. E-mail: martin.olazar@ehu.es.
[†] Departamento de Ingeniería Química.
[‡] Departamento de Ingeniería Química y Medio Ambiente.

10.1021/ie800376d CCC: $40.75
Published on Web 09/10/2008

they are related to studies in thermobalance,[35] and to the reforming of thermal pyrolysis volatile products in a fixed bed reactor,[36−39] or fluidized bed reactor.[40]

Experimental Section

Tire Material. The main components of the tire studied are (in wt %): natural rubber (SMR 5CV), 29.59; styrene−butadiene rubber (SBR 1507), 29.59; carbon black (ISAF N220), 29.59. Other components are (in wt %) as follows: stearic acid, 0.59; *n*-isopropyl-*n*′-phenyl-*p*-phenylenediamine, 0.89; zinc oxide, 2.96; phenolic resin, 2.37; sulfur, 0.89; *n*-cyclohexyl-2-benzothiazole-sulfenamide, 0.89; hexamethylentetramine (H-7), 0.18; (*n*-cyclohexylthio)phthalimide, 0.12; aromatic oil, 2.37. The density is 1140 kg m^{-3}, and the high calorific value (determined in a Parr 1356 isoperibolic bomb calorimeter) is 38847 kJ kg^{-1}.

Catalysts. The two catalysts used have been prepared based on ZSM-5 and HY zeolites, which have been supplied by Zeolyst International. In order to attain a suitable particle size and mechanical resistance (which is required to minimize the loss of material by attrition), natural bentonite (Exaloid) has been used as binder (30 wt %) and fused alumina (Martinswerk) as inert (45 wt %), thereby increasing the thermal stability of the catalyst.

The ZSM-5 zeolite has been supplied in ammonium form and is calcined at 550 °C prior to mixing with alumina and bentonite in order to obtain the definitive acid form (HZSM-5). The bentonite has been supplied in sodium form and is mixed with a NH_4NO_3 dissolution to obtain the ammonium form. The HY zeolite has been supplied in acid form, and so no acidification step is required.

The catalyst is prepared by mixing bentonite with alumina and zeolite in distilled water, which produces a paste. Once the mixture has been homogenized, the excess water is filtered and the paste is extruded through holes of 0.5−1.5 mm diameter. The extrudates are dried for 24 h at ambient temperature and subsequently ground and sieved, and the fraction with a particle diameter between 0.3 and 1 mm is chosen. This fraction is dried at 110 °C for 24 h and subsequently calcined at 575 °C for 2 h (this temperature is reached at a rate of 5 °C min^{-1}). The calcination temperature of the catalyst, 575 °C, has been established in order to reach a balance between initial activity and catalyst stability (resistance to irreversible deactivation by dealumination).[41] Prior to use, the prepared catalyst is always calcined at 550 °C for 2 h.

The physical properties of the fresh catalysts and of those used for different values of time on stream have been determined from the results of N_2 adsorption−desorption obtained in a Micromeritics ASAP 2000 apparatus. The acid strength distribution has been determined by combining the calorimetric and thermogravimetric measurements of NH_3 differential adsorption at 150 °C, using a Setaram TG-DSC 111 calorimeter connected online to a Balzers Thermostar mass spectrometer. Likewise, the same equipment is used to determine the curves of temperature-programmed desorption (TPD) of NH_3.[42,43]

The characterization of the carbonaceous material (carbon black and catalytic coke) has been carried out by combustion at programmed temperature (TPO) in the same equipment used for catalyst acidity measurement, by monitoring the masses 18, 28, and 44 for water, CO, and CO_2, respectively.

Reaction Equipment. Figure 1 shows a scheme of the pyrolysis unit, which is made up of the following components: (1) solid feeding system; (2) inert gas feeding system; (3) pyrolysis reactor; (4) a system for removing fines from the gaseous stream; (5) condensers and filter for collecting liquid product; (6) a system for analyzing the volatile compounds by chromatography; (7) control system (LABTECH program under Windows).

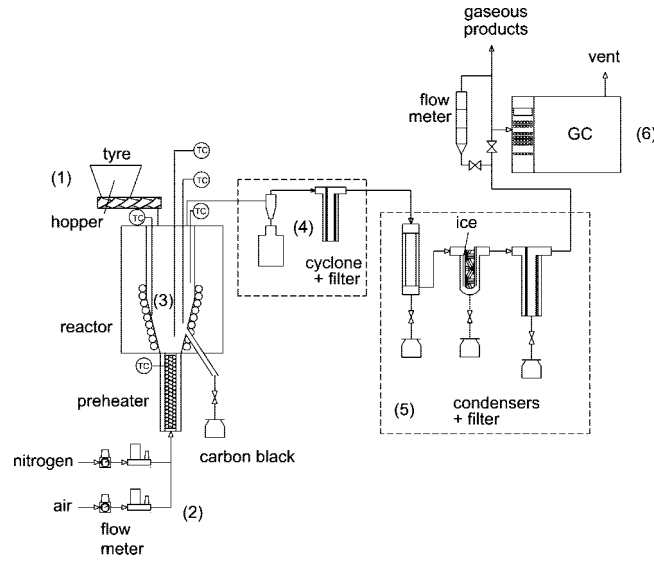

Figure 1. Scheme of the pyrolysis unit.

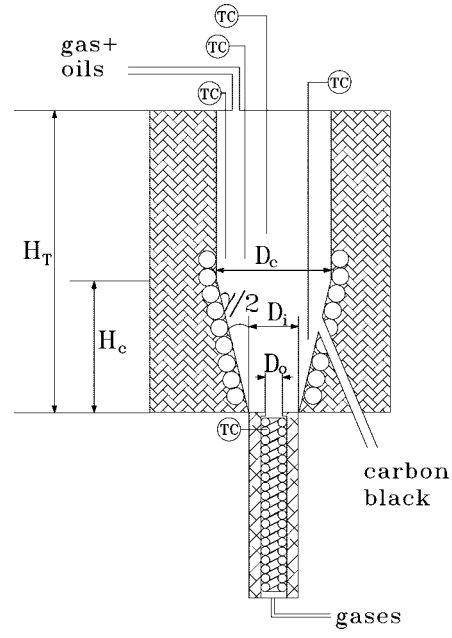

Figure 2. Scheme of the pyrolysis reactor.

Figure 2 shows a scheme of the reactor, which is of conical geometry with an upper cylindrical section. The total height of the reactor, H_T, is 34 cm, the height of the conical section, H_c, 20.5 cm, and the angle of the conical section, γ, 28°. The cylindrical section diameter, D_c, is 12.3 cm, the base of the reactor, D_i, 2 cm, and the gas inlet diameter, D_o, 1 cm. The mass of catalyst + sand is between 30 and 100 g, and under reaction conditions, the bed of solids is in the conical section of the reactor. These dimensions guarantee bed stability in a wide range of process conditions, particularly those concerning gas velocity, and they have been established in previous hydrodynamic studies.[44−46] The hydrodynamic regime may vary from the spouted bed to a vigorous jet spouted bed (or dilute spouted bed), with a wide transition regime between both.[47] This implies great versatility in the gas−solid contact conditions,

especially in the gas residence time, given that by starting at a given stagnant bed height, H_o, and increasing the inert gas velocity, the gas residence time may be decreased from a few seconds to values close to 20 ms.[48]

There is a cartridge below the reactor containing a ceramic resistance, which is inside a metal casing and thermally insulated. This resistance heats the nitrogen stream to the reaction temperature, which is measured with a thermocouple placed at the upper end of the resistance (below the reactor inlet). In the conical section of the reactor, there is another resistance surrounding the wall of this section, which is controlled by measuring the temperature at a point near the wall by means of another fixed thermocouple. Furthermore, the reactor is insulated in order to minimize energy consumption. In addition to the two fixed thermocouples, the unit is provided with a multipoint thermocouple, which allows for simultaneously taking five temperature readings at several bed levels in the same radial position.

In order to retain fine carbon black particles entrained by the volatile products, a high-efficiency cyclone followed by a 25-μm sintered steel filter was placed at the reactor outlet, both within a hot box to avoid volatile condensation. The gases leaving this filter circulate through a volatile condensation system consisting of a double-shell tube cooled by tap water. The gaseous stream is then passed through another 25-μm sintered steel filter, where the small drops that are not condensed are retained. There is a bubble flowmeter at the outlet of the filter for recording the flow rate of noncondensable gases.

Product Analysis. Identification of the volatile products has been carried out by GC/MS in a Shimadzu QP2010S using a NIST library. The chromatograph is provided with a TRB-1 column (20 m × 0.10 mm). Product quantification has been carried out by gas chromatography using two pieces of equipment, one for noncondensable gases and the other one for condensed liquids. The equipment for noncondensable gas analysis is an Agilent microGC 3000 provided with three analytical channels: (i) a channel with Plot U precolumn (3 m × 0.32 mm) and Plot molecular sieve 5A capillary column (10 m × 0.32 mm), for permanent gases, and (ii) two channels with Pora Plot Q capillary column (10 m × 0.32 mm), one for oxygenate compounds and the other one for light hydrocarbons (up to C_4). The condensed liquid product has been analyzed by GC/MS in the same equipment used for product identification.

Results

Yields and Product Composition. Figure 3 compares the yields of the different product fractions obtained by thermal and catalytic pyrolysis carried out at 425 °C (graph a) and 500 °C (graph b). The results have been obtained by feeding pulses of 2 g of tire/min into a 15-g catalytic bed (the mass of sand + catalyst in the bed is 30 g). The following fractions of volatile products have been monitored: C_1-C_4 gases (with CO and CO_2), nonaromatic C_5-C_{10}, aromatic C_{10-} and C_{10+} (tar). In view of the results, the catalyst and operating temperature are clearly the key variables in the pyrolysis of tires, for obtaining high selectivity toward interesting products.

As observed in Figure 3a, the yield of the gaseous fraction at 425 °C is higher in catalytic pyrolysis than in thermal pyrolysis. Thus, the higher gaseous yield, 7.56%, is obtained with the HZSM-5 zeolite catalyst, whereas the HY zeolite catalyst gives a yield of 3.34%.

The difference in the results between the two catalysts is significant at 500 °C (Figure 3b). The yield with the HZSM-5 zeolite catalyst is very high, 19.32%, whereas with the HY zeolite it is lower, 2.49%, than that obtained at 425 °C using the HZSM-5 zeolite catalyst and that obtained at 500 °C in thermal pyrolysis. These results explain why an increase in temperature favors HZSM-5 zeolite catalyst capacity for cracking heavy fractions, whereas the HY zeolite catalyst favors alkylation and aromatization of C_1-C_4 fraction components to give heavier fraction components. This different performance by the catalysts is due to the different shape selectivity of the zeolites. Another interesting fact is the higher hydrogen-transfer capacity of the HY zeolite.

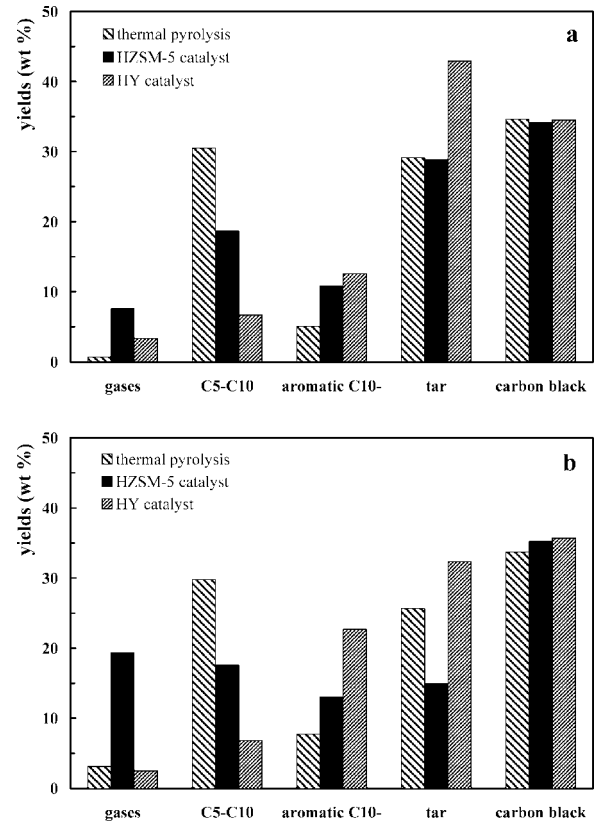

Figure 3. Effect of the catalyst on the yields (wt %) of product fractions. Graph a, 425 °C. Graph b, 500 °C.

The use of the catalyst gives way to a significant decrease in the yield of the nonaromatic C_5-C_{10} fraction. The yield of this fraction at 425 °C (Figure 3a), which is 30.49% in thermal pyrolysis, decreases to 18.65% with the HZSM-5 zeolite catalyst and to 6.68% with its HY counterpart. At 500 °C (Figure 3b), the yield of the nonaromatic C_5-C_{10} fraction decreases from 29.80% in thermal pyrolysis to 17.56 and 6.81% with HZSM-5 and HY zeolite catalysts, respectively. As noted earlier, the causes for the decrease in this fraction are as follows: (i) for the HZSM-5 zeolite catalyst, the cracking to the gaseous fraction, and (ii) for the HY zeolite catalyst, the condensation to heavier components.

Contrary to the result obtained for nonaromatic hydrocarbons, the yield of the aromatic C_{10-} fraction is favored using both catalysts. At 425 °C (Figure 3a), the yield increases from 5.07% in thermal pyrolysis to 10.82% with the HZSM-5 zeolite catalyst and to 12.57% with its HY zeolite counterpart. An increase in temperature heightens the effect of the catalysts, and at 500 °C (Figure 3b), the yield of the aromatic C_{10-} fraction increases from 7.77% in thermal pyrolysis to 13.00% with the HZSM-5 zeolite catalyst and to 22.67% with its HY counterpart. These results are evidence of the aromatization capacity of the HY zeolite, which is higher than that of the HZSM-5 zeolite.

There is also a significant difference in the results obtained with the two catalysts for the tar fraction yield. At 425 °C (Figure 3a), the higher yield has been obtained with the HY catalyst, 42.91%, compared to 29.12% obtained in thermal pyrolysis and to 28.87% obtained with the HZSM-5 catalyst. An increase in temperature contributes to decreasing the tar yield, which is 25.64% in thermal pyrolysis at 500 °C (Figure 3b) and 32.33% with the HY catalyst at the same temperature. It is noteworthy that this yield is much lower, 14.92%, with the HZSM-5 zeolite catalyst. In fact, it is the lowest yield obtained in the runs carried out. This result is specially interesting for decreasing tar content and should be attributed to steric limitations in the channels of the HZSM-5 zeolite for locating structures larger than single-ring molecules.

There are no significant differences in the yields of carbon black, and the slight increase observed when catalysts are used at 500 °C (Figure 3b) is explained by the deposition of carbonaceous material obtained by polycondensation of high molecular volatiles, which is activated by acid catalysts.

These results concerning the use of the catalyst in situ and the effect of temperature are consistent with those of other authors in the reforming of the volatile stream on acid catalysts,[36−39,49] although the different technological conditions should be considered in the comparison. Thus, the concentrations of the volatile fractions in the spouted bed reactor are lower than those of the fixed or fluidized bed, and a tire/catalyst ratio (tire mass fed in a run by catalyst mass unit) lower than in catalytic reforming has been used, which explains the high yield of tar obtained in this paper.

Figure 4 shows the effect of using the catalyst on gas composition at 425 (graph a) and 500 °C (graph b). As observed, the use of the catalyst increases the yield of most components and the HZSM-5 zeolite catalyst is more efficient. The yields of ethene, propene, 1,3-butadiene, 2-butene, and butane are especially noteworthy. Except the latter, the remaining are olefins, which indicates that both acid catalysts promote the reactions for their formation. A high selectivity to propene and butadiene with the catalyst prepared based on the HZSM-5 zeolite is noteworthy, which is a well-known feature attributed to the shape selectivity of this zeolite that favors monomolecular cracking.[50−52] The high selectivity to these products with the HZSM-5 zeolite catalyst has also been observed by Williams and Brindle.[53] It should be noted that the catalyst with the HY zeolite has considerable activity for butadiene transformation at 500 °C, given that the yield of this compound is lower than in thermal pyrolysis. This reaction takes place thanks to the hydrogen-transfer capacity of the HY zeolite, which favors Diels−Alder condensation reactions for aromatic generation.

Figure 5 compares the yields for the components in the nonaromatic C_5-C_{10} fraction. In this case, the effect of the catalyst on the C_{10} lump yield should be noted, given that this yield is very high in thermal pyrolysis, 28.01% at 425 °C and 22.08% at 500 °C, but significantly decreases when using the catalysts. The HY zeolite catalyst decreases this yield to 2.32% at 425 °C and to 3.72% at 500 °C. With the HZSM-5 zeolite catalyst the decrease is lower, 7.42% at 425 °C and 4.63% at 500 °C.

The main component in the C_{10} lump is limonene, whose yield at 425 °C decreases from 23.93% in thermal pyrolysis to 5.51% with the HZSM-5 zeolite catalyst and to 1.99% with the HY zeolite catalyst. At 500 °C, the yield of limonene decreases from 16.94% in thermal pyrolysis to 3.78% with the HZSM-5 zeolite catalyst and to 2.37% with the HY zeolite catalyst.

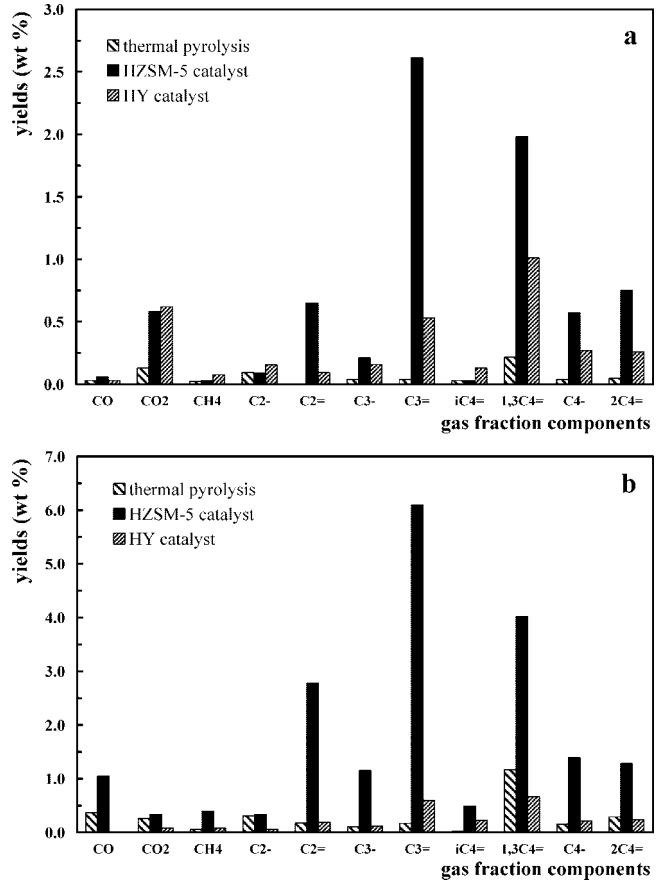

Figure 4. Effect of the catalyst on the yields (wt %) of the components in the gaseous fraction. Graph a, 425 °C. Graph b, 500 °C.

At 425 °C, and due to the mild catalytic cracking of higher carbon atom number lumps, the yields of C_5-C_7 lumps are higher in catalytic pyrolysis than in thermal pyrolysis. At 500 °C, the cracking is more severe and also affects C_7-C_9 lumps, and consequently, their yield decreases, although the temperature is higher.

As is observed in Table 1, the catalysts significantly increase the yields of BTX (benzene, toluene, xylenes), ethylbenzene, and styrene. These are the main components obtained with the HZSM-5 zeolite catalyst. The yield of aromatic C_{10-} is higher with the HY zeolite catalyst, due to the formation of 1-methyl-4-(1-methylethyl)benzene, 2,3-dihydro-4-methyl-1*H*-indene, 1-ethenyl-3-ethylbenzene, 1-etheny-4-ethylbenzene, and 2,3,4-tetramethylbenzene. These components are of great commercial interest, particularly the xylenes, and the HZSM-5 zeolite catalyst at 500 °C has produced yields of 1.65, 3.35, and 4.08% for benzene, toluene, and xylenes, respectively. These yields are slightly lower than those obtained in the reforming of thermal pyrolysis products.[36]

The yields of the tar lump obtained with the two catalysts are compared in Figure 6 at 425 °C (graph a) and 500 °C (graph b). It is noteworthy that the HY zeolite catalyst produces a high yield of aromatic compounds in the tar (31.24% at 425 °C and 25.15% at 500 °C), at the expense of a decrease in the yield of nonaromatics (∼2.4% at 425 °C and ∼1.7% at 500 °C), which is due to condensation reactions favored by a temperature increase. This capacity for condensation and alkylation confirms the results of catalytic reforming with the HY zeolite.[37−39]

The different results obtained with HZSM-5 and HY zeolite catalysts are due to the difference in shape selectivity between the zeolites. The greater micropore size of the HY zeolite and

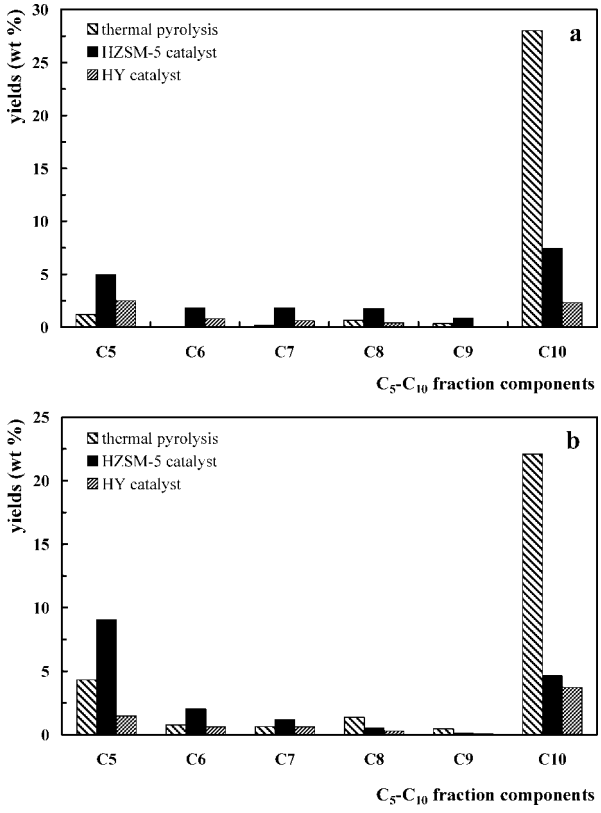

Figure 5. Effect of the catalyst on the yields (wt %) of the components in the nonaromatic C_5-C_{10} fraction. Graph a, 425 °C. Graph b, 500 °C.

its hydrogen-transfer capacity largely explain the yields and composition of volatile products. It should be noted that other potentially important catalyst properties, such as total acidity or acid site strength, are not significantly different between the two catalysts.

A study has been carried out in another complementary paper concerning the effect on the conditions of this catalytic process on the composition and properties of the products (gas, liquid, and residual carbon black), and the interest for upgrading these fractions as fuels or raw materials is assessed.[54]

Deterioration of Catalyst Properties. The properties of the fresh catalysts and of those used under different conditions in runs of different durations are set out in Table 2. These runs have been carried out by feeding 1-g pulses of tire base material per minute, until the total amount indicated in the table has been fed in the run. The reactor operates in a discontinuous regime for the catalyst (the amounts used are 15, 50, and 100 g), which is maintained in the bed up to the end of the run. The micropore size of the fresh catalysts is characteristic for each zeolite (5.6 Å for HZSM-5 and 7.8 Å for HY). The bentonite and the alumina formed the matrix where the zeolite is embedded, and they provide mesopores (inherent to each one of these materials) and macropores (voids between material particles), which contribute to attenuating deactivation in the zeolite micropores. As a result of the agglomeration process, the contribution of micropore volume is greater in the HY zeolite catalyst (7.6%). Furthermore, the contribution of macropores is significantly higher in the HZSM-5 zeolite catalyst (74.7%), whereas the HY zeolite catalyst is more mesoporous (24.5%). As observed in Table 2, the properties of the used catalysts are significantly deteriorated. Mesopore volume is an exception, which is almost constant or undergoes a slight decrease. In order to explain this phenomenon, it should be noted that the carbon black deposited

Table 1. Yields (in wt %) of Components in the Aromatic $C_{10}-$ Fraction for Both Catalysts (15 g of Catalyst), at 425 and 500 °C

		HZSM-5		HY	
		425 (°C)	500 (°C)	425 (°C)	500 (°C)
C_6		0.55	1.65	0.35	0.24
	benzene	0.55	1.65	0.35	0.24
C_7		1.91	3.35	0.52	0.64
	toluene	1.91	3.35	0.52	0.64
C_8		4.53	5.23	1.16	1.98
	ethylbenzene	0.80	0.78	0.49	1.28
	xylenes	2.55	4.08	0.67	0.08
	styrene	1.18	0.37	0.00	0.62
C_9		2.52	1.59	1.69	3.25
	1-methylethylbenzene	0.11	0.03	0.25	0.13
	1-propenylbenzene	0.06	0.00	0.00	0.00
	propylbenzene	0.20	0.03	0.16	0.12
	1-ethyl-3-methylbenzene	0.00	0.21	0.55	0.69
	1- ethyl −2-methylbenzene	0.89	0.51	0.05	0.56
	α-methylstyrene	0.62	0.44	0.23	0.36
	1,2,3-trimethylbenzene	0.50	0.15	0.45	1.39
	indene	0.14	0.22	0.00	0.00
C_{10}		1.31	1.18	8.85	16.56
	1-methyl-2-(methylethyl)benzene	0.31	0.19	0.11	0.50
	1-methyl-4-(1-methylethyl)benzene	0.00	0.00	0.78	1.24
	1-methyl-4-propylbenzene	0.16	0.00	0.22	0.86
	1-methyl-2-propylbenzene	0.00	0.00	0.00	0.05
	2-ethyl-1,4-dimethylbenzene	0.00	0.00	0.15	0.80
	1-ethenyl-3-ethylbenzene	0.00	0.00	1.17	3.28
	1-ethenyl-4-ethylbenzene	0.00	0.00	1.75	2.21
	1,2-diethylbenzene	0.23	0.01	0.00	0.00
	2-methyl-1-methylethenylbenzene	0.27	0.18	0.00	0.00
	1,2,4,5-tetramethylbenzene	0.00	0.09	0.61	1.48
	1,2,3,4-tetramethylbenzene	0.00	0.00	0.94	0.92
	1-methyl-2-cyclopropen-1-ylbenzene	0.16	0.00	0.00	0.00
	2-methyl-1*H*-indene	0.00	0.18	0.00	0.00
	3-methyl-1*H*-indene	0.12	0.13	0.00	0.00
	1,4,5,8-tetrahydronaphthalene	0.02	0.18	0.00	0.48
	naphthalene	0.04	0.08	2.26	3.04
	2,3-dihydro-4-methyl-1*H*-indene	0.00	0.14	0.86	1.70
total		10.82	13.00	12.57	22.67

on the mesopores and on the outside of the particles has certain mesoporosity.[55]

Figure 7 shows that BET surface area and micropore volume (limiting properties for the access of volatile components to the active sites) decrease as the amount of material treated per mass unit of catalyst is increased. The results correspond to the HZSM-5 zeolite catalyst. It is observed that both properties have a decreasing trend, which is more pronounced for small amounts of material treated per mass unit of catalyst, which is attributed to the fouling of catalyst pores by carbon black. Although only two points (fresh and used catalyst) are available for the HY zeolite catalyst, a decrease of both properties is appreciated, which is even more pronounced than that for the HZSM-5 zeolite catalyst. The BET surface of the HY zeolite catalyst decreases from 221 to 90 $m^2\ g^{-1}$ for 7.5 g of tire fed/g of catalyst (tire/catalyst = 7.5) and that of the HZSM-5 zeolite catalyst decreases from 182 to ~100 $m^2\ g^{-1}$. The micropore volume undergoes 68% decrease in the HY catalyst and 50% in the HZSM-5 for the same tire/catalyst ratio.

Figure 8 shows the results obtained for acidity in the HZSM-5 zeolite catalyst (graph a) and the HY zeolite catalyst (graph b), fresh and used. Acidity steadily decreases as the amount of material treated by mass unit of catalyst is increased, although the used catalysts maintain considerable total acidity, particularly the HZSM-5 zeolite catalyst, for which this property decreases less than for the HY zeolite catalyst.

Concerning the effect of acid strength, the HZSM-5 zeolite catalyst (graph a) undergoes a slight decrease from 140−150

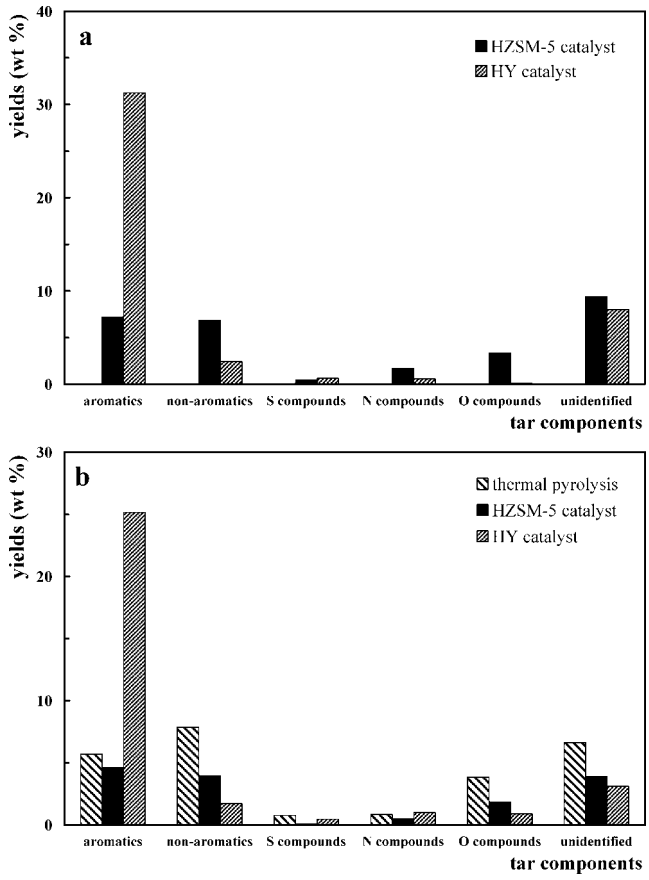

Figure 6. Effect of the catalyst on the yields of tar components. Graph a, 425 °C. Graph b, 500 °C.

to 130−140 kJ (mol of NH_3)$^{-1}$. This decrease is similar for the HY zeolite catalyst (graph b).

Figure 9 compares NH_3 TPD for the fresh catalysts and those used at different times on stream values. Although the deterioration of total acidity (area under the curve) is considerable for both catalysts, Figure 9a, corresponding to the HZSM-5 zeolite catalyst, shows that a high level of strong acidity is maintained (peak at 350 °C) until a high amount of tire is fed by catalyst mass unit (tire/catalyst = 10.9). The contribution of very strong acidity is lower in the fresh HY zeolite catalyst (graph b), and for this catalyst, both total acidity and site strength undergo a clear decrease, which is confirmed as the temperature corresponding to the sole TPD peak shifts to lower values as catalyst is used longer.

Deposition of Coke-Carbon Black on the Catalyst. Visual observation of the used catalyst particles reveals that they are covered by a black carbonaceous layer. This layer partially comes off by slight stirring, almost certainly due to particle collisions during the reaction when the layer reaches its maximum possible size. Combustion of the carbonaceous matter remaining in the particles (subsequent to removing the external carbon black by stirring) performed in a thermobalance at programmed temperature (TPO) shows that the carbonaceous material deposited includes the following: (i) carbon black that is externally covering the catalyst particles and that deposited on the catalyst macropores and mesopores and (ii) coke or carbonaceous material deposited on the catalyst micropores (in the zeolite), which is of catalytic origin and blocks the acid sites and may potentially deactivate cracking capacity. Table 3 shows the yields of these coke-carbon blacks (total carbonaceous matter) and contents in the catalysts for different experimental conditions. This content is determined in weight percent by mass unit of catalyst.

Figure 10 shows the evolution of coke-carbon black content deposited on the catalyst as the amount of tire fed is increased. The results show that the carbonaceous material deposited linearly increases with operation time and amount of tire treated. In principle, the amount of coke deposited on the zeolite micropores significantly contributes to the difference in the total amount of carbonaceous material between the two catalysts, given that this content is higher in the HY zeolite catalyst. It is accepted in the literature that micropore intersection supercages in the HY zeolite allow for condensation of coke precursors toward polymeric structures, which is favored by high acid strength sites. Nevertheless, coke formation in HZSM-5 zeolite is hindered by several factors: (1) there is a higher shape selectivity of micropore channels; (2) the intersections between channels do not generate additional locations for large molecule blockage; (3) the sites have a moderate and homogeneous acid strength; (4) hydrogen-transfer capacity is low, which hinders aromatization and condensation Diels−Alder reactions.[56,57] This higher capacity for coke formation in the HY zeolite catalyst is reflected in the yield of carbonaceous material, which is between 4.4 and 4.7% for the HY zeolite catalyst and between 3.0 and 3.6% for the HZSM-5 zeolite catalyst (Table 3).

The higher coke content within the HY zeolite catalyst is consistent with the results by Williams and Brindle,[36] which are obtained in a catalytic reaction in series with thermal pyrolysis reactor and for a catalyst/tire ratio of 1. According to these authors, coke content increases from 7.2% at 430 °C to 8% at 600 °C for the HY zeolite catalyst, whereas for the HZSM-5 zeolite catalyst coke content increases from 4% at 430 °C to 7.6% at 600 °C.

The results in Figure 10 have been obtained by TPO carried out on the carbonaceous material deposited on the catalysts. As an example, Figure 11 shows the TPO curves and those obtained by monitoring CO, CO_2, and H_2O in the mass spectrometer for the two catalytic beds, 100 g of HZSM-5 zeolite catalyst (Figure 11a) and 15 g of HY zeolite catalyst (Figure 11b). Figure 12 shows the results for carbon black combustion, which have been carried out to identify this material from the whole carbonaceous material deposited on the catalyst.

Table 2. Physical Properties of the Fresh Catalysts and Once They Have Been Used under Different Conditions

	HZSM-5				HY	
	fresh	15 g	50 g	100 g	fresh	15 g
amount fed (g)		163	225	66		112
tire fed (g)/g catalyst		10.9	4.5	0.66		7.5
temperature (°C)		425	500	500		500
BET surface area (m^2/g)	182	93	111	144	221	90
micropore surface area (m^2/g)	87	32	64	76	127	40
mesopore surface area (m^2/g)	94	60.5	48	68	95	50
micropore volume (cm^3/g)	0.039	0.014	0.028	0.033	0.053	0.017
mesopore volume (cm^3/g)	0.16	0.14	0.09	0.12	0.17	0.12

Table 3. Results of Coke-Carbon Black Deposited on the Catalyst under Different Operating Conditions

catalyst	mass (g)	T (°C)	tire fed (g)	g_{tire}/g_{cat}	yield (wt %)	coke-carbon black (wt %)
HZSM-5	100	500	123	1.23	3.6	4.4
HZSM-5	100	500	66	0.66	3.2	2.1
HZSM-5	50	500	107	2.14	3.0	6.3
HZSM-5	15	500	68	4.53	3.2	14.3
HZSM-5	15	425	163	10.87	3.5	37.5
HY	50	500	84	1.68	4.7	7.9
HY	15	500	112	7.47	4.5	33.8
HY	15	425	103	6.87	4.4	29.9

Two differentiated peaks are observed in Figure 11. A comparison with carbon black combustion (Figure 12) allows for establishing that the first peak (at 475 °C) corresponds to the coke deposited within the micropores of the catalyst. This coke is lighter and has a higher H/C ratio than carbon black and, consequently, burns faster. The peak corresponding to carbon black combustion in Figure 11 (∼540 °C), which is similar to that in Figure 12, masks the peak corresponding to the catalytic coke combustion when the content of this coke is low (as is the case in Figure 11) compared to the total amount (29.9%). Furthermore, the catalytic coke deposited in the HY zeolite will presumably be more condensed than that corresponding to HZSM-5 zeolite, due to the easier evolution of the coke in the HY zeolite, which is attributable to the larger micropore diameter and higher hydrogen transfer capacity of this zeolite.[57]

From the measurement of yield evolution with time on stream, it has been proven that the kinetic behavior of both catalysts remains unchanged, without significant deactivation, at least under the reaction conditions studied: up to 6.87 g of tire treated/g of HY zeolite catalyst and 10.87 g/g of HZSM-5 zeolite catalyst. The explanation why this result apparently contradicts the deterioration observed in the physical properties and acidity of the catalyst may be attributed to the following: (i) the higher porosity of carbon black under pyrolysis conditions than under those used in the analysis; (ii) the suitable preparation of the catalyst (by agglomerating the catalyst with bentonite and alumina) with a macroporous and mesoporous matrix that allow for "storing" the carbonaceous matter without blocking the zeolite micropores; (iii) the relatively low accumulated amount of tire fed by mass unit of catalyst, which advises extending this study on deactivation to higher values of time on stream.

In addition to insignificant deactivation (for low values of time on stream), it has also been proven that the catalysts fully recover their physical properties and acidity subsequent to combustion of the carbonaceous matter with air at 550 °C. This guarantees that the catalyst is useful for uninterrupted reaction−regeneration cycles, which is essential for process viability.

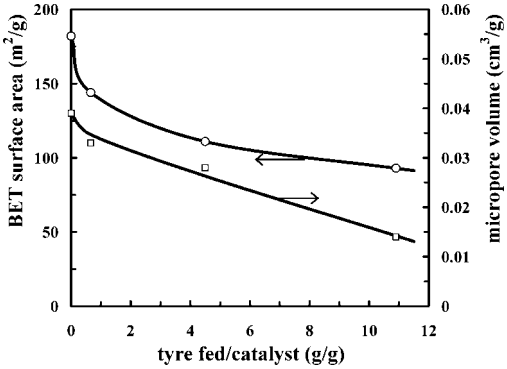

Figure 7. Effect of the amount of tire treated on the deterioration of the HZSM-5 zeolite catalyst physical properties.

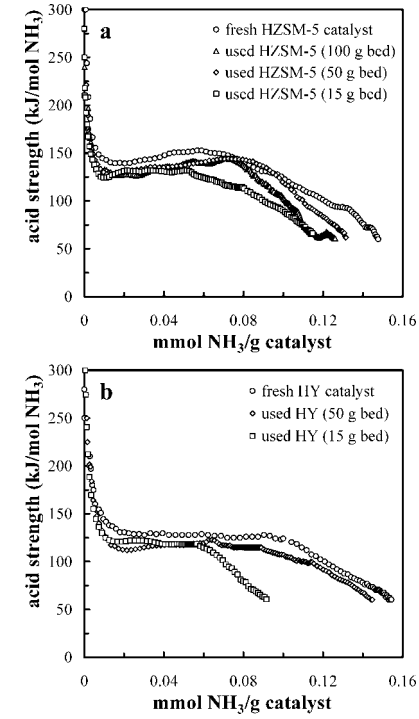

Figure 8. Comparison of acid strength distribution of fresh catalysts and those used under different operating conditions (Table 3). Graph a, HZSM-5 zeolite catalyst. Graph b, HY zeolite catalyst.

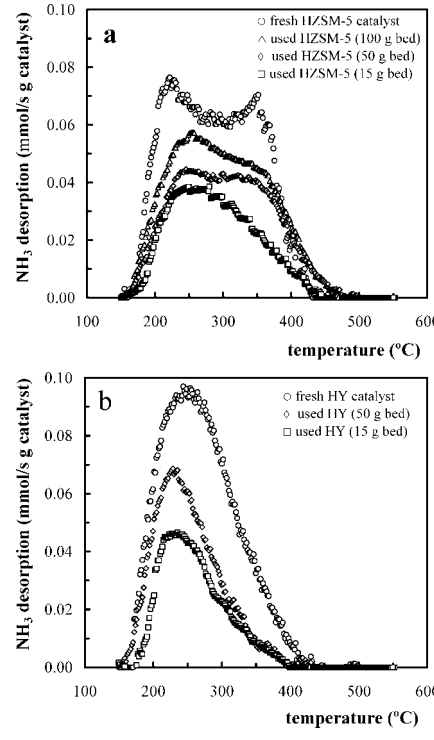

Figure 9. Comparison of NH_3 TPD of fresh catalysts and those used under different operating conditions. Graph a, HZSM-5 zeolite catalyst. Graph b, HY zeolite catalyst.

Conclusions

The conical spouted bed reactor is suitable for tire pyrolysis using in situ catalysts. Operation may be carried out in a wide

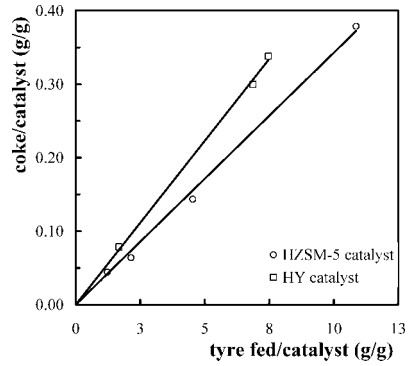

Figure 10. Evolution of coke-carbon black content in the catalyst with the amount of tire treated.

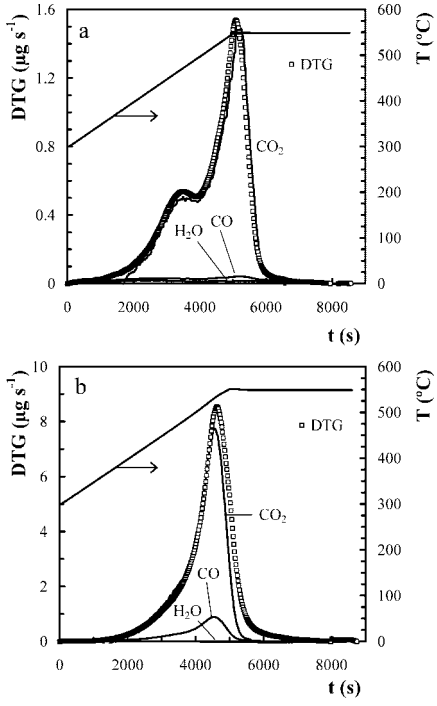

Figure 11. Weight loss of coke-carbon black (DTG) and formation of combustion gases (CO, CO_2, and H_2O). Graph a: HZSM-5 zeolite catalyst (100 g); tire fed, 123 g; 500 °C. Graph b: HY zeolite catalyst (15 g); tire fed, 103 g; 425 °C.

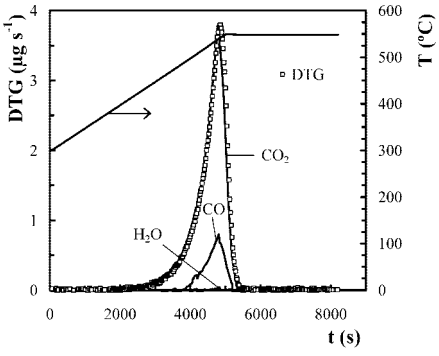

Figure 12. Weight loss (DTG) in the combustion of carbon black and formation of combustion gases (CO, CO_2, and H_2O).

range of conditions, without problems of stability, segregation, or bed agglomeration. The use of acid catalysts allows for significantly modifying the yields of volatile fractions, in order to increase their value added as chemicals or fuels.

The use of an acid catalyst gives way to an increase in the yield of gases. It should be noted that a high yield of propylene and butane is obtained with the HZSM-5 zeolite catalyst, whereas the use of the HY zeolite catalyst produces condensation of butadiene to higher molecular weight structures.

The catalyst decreases the yield of the nonaromatic C_5-C_{10} fraction and favors the cracking of d-limonene to form C_5-C_7 compounds. A high BTX yield is produced with the HZSM-5 zeolite catalyst, particularly that of xylenes (4.08%) at 500 °C.

The increase in temperature from 425 to 500 °C increases HZSM-5 zeolite capacity for cracking and HY zeolite for condensation. This effect is interesting, given that, by using the HZSM-5 zeolite catalyst at 500 °C, the yield of tar attenuates considerably, due to hindrance by this zeolite shape selectivity.

The comparison of catalysts reveals their different performance, which is inherent to the properties of the corresponding zeolites, especially shape selectivity and hydrogen-transfer capacity. Thus, HZSM-5 zeolite activates the cracking toward C_1-C_4 gases and has limited capacity for condensation toward polyaromatic structures, which explains the high selectivity to BTX and the generation of a small amount of tar. HY zeolite has a high capacity for BTX alkylation and for condensation (especially olefins and aromatics) toward tar components.

The analysis of the used catalysts shows a significant deterioration of properties, although the HZSM-5 zeolite catalyst undergoes a smaller deterioration, with a decrease in surface area from 182 to ~100 $m^2\ g^{-1}$ when 7.5 g of tire/g of catalyst has been fed, and with 50% decrease in micropore volume. This deterioration of physical properties is more significant than the decrease in both total acidity and acid strength of catalyst active sites.

The results of combustion of the carbonaceous material deposited on the catalyst allow for distinguishing the material (carbon black) externally coating the catalyst particles, and also filling bentonite and alumina mesopores, from the coke deposited on the zeolite micropores, which is of catalytic origin and whose formation (by condensation of heavy hydrocarbons) is more favored in the supercages of HY zeolite than in HZSM-5 zeolite intersections. The small hydrogen transfer of HZSM-5 zeolite contributes to its better performance.

The deterioration of physical properties observed by conventional analysis is insufficient for a significant loss of activity in the range of time on stream studied, which may be attributed to the fact that under the reaction conditions studied the residual carbon black deposited on the catalysts does not block the catalyst micropores. Blockage would occur for high levels of deposition in the catalyst meso- and macropores.

Acknowledgment

This work was carried out with the financial support of the University of the Basque Country (Project GIU06/21), the Ministry of Science and Education of the Spanish Government (Project CTQ2004-01562/PPQ), the Ministry of Environment of the Spanish Government (Project 242/2006/2-5.3), and the Department of Industry of the Basque Government (Project IE05-149).

Literature Cited

(1) Larsen, M. B.; Schultz, L.; Glarborg, P.; Skaarup-Jensen, L.; Dam-Johansen, K.; Frandsen, F.; Herriksen, U. Devolatilization characteristics of large particles of tyre rubber under combustion conditions. *Fuel* **2006**, *85*, 1335–1345.

(2) Sunthonpagasit, N.; Duffey, R. Scrap tires to crumb rubber: feasibility analysis for processing facilities. *Resour., Conserv. Recycl.* **2004**, *40*, 281–299.

(3) Huffman, G. P.; Shah, N. Can waste plastics and tires be recycled economically. *CHEMTECH* **1998**, *28*, 34–43.

(4) Sharma, V. K.; Fortuna, F.; Macarini, M.; Berillo, M.; Cornacchia, G. Disposal of waste tyres for energy recovery and safe environment. *Appl. Energy* **2000**, *65*, 381–394.

(5) de Marco, I.; Laresgoiti, M. F.; Cabrero, M. A.; Torres, A.; Chomón, M. J.; Caballero, B. Pyrolysis of scrap tyres. *Fuel Process. Technol.* **2001**, *72*, 9–22.

(6) González, J. F.; Encinar, J. M.; Canito, J. L.; Rodríguez, J. J. Pyrolysis of automobile tyre waste. Influence of operating variables and kinetics study. *J. Anal. Appl. Pyrolysis* **2001**, *58*, 667–683.

(7) Laresgoiti, M. F.; de Marco, I.; Torres, A.; Caballero, B.; Cabrero, M. A.; Chomón, M. J. Chromatographic analysis of the gases obtained in tyre pyrolysis. *J. Anal. Appl. Pyrolysis* **2000**, *55*, 43–54.

(8) Laresgoiti, M. F.; Caballero, B.; de Marco, I.; Torres, A.; Cabrero, M. A.; Chomón, M. J. Characterization of the liquid products obtained in tyre pyrolysis. *J. Anal. Appl. Pyrolysis* **2004**, *71*, 917–934.

(9) Berrueco, C.; Esperanza, E.; Mastral, F. J.; Ceamanos, J.; García-Bacaicoa, P. Pyrolysis of waste tyres in an atmospheric static-bed batch reactor: Analysis of the gases obtained. *J. Anal. Appl. Pyrol.* **2005**, *74*, 245–253.

(10) Ucar, S.; Karagoz, S.; Ozkan, A. R.; Yanik, J. Evaluation of two different scrap tires as hydrocarbon source by pyrolysis. *Fuel* **2005**, *84*, 1884–1892.

(11) Williams, P. T.; Besler, S.; Taylor, D. T. The pyrolysis of scrap automotive tyres: The influence of temperature and heating rate on product composition. *Fuel* **1990**, *69*, 1474–1482.

(12) Lee, J. M.; Lee, J. S.; Kim, J. R.; Kim, S. D. Pyrolysis of waste tires with partial oxidation in a fluidized-bed reactor. *Energy* **1995**, *20*, 969–976.

(13) Wey, M. Y.; Huang, S. C.; Shi, C. L. Oxidative pyrolysis of mixed solid wastes by sand bed and freeboard reaction in a fluidized bed. *Fuel* **1997**, *76*, 115–121.

(14) Kaminsky, W.; Mennerich, C. Pyrolysis of synthetic tire rubber in a fluidised-bed reactor to yield 1,3-butadiene, styrene and carbon black. *J. Anal. Appl. Pyrolysis* **2001**, *58*−*59*, 803–811.

(15) Roy, C.; Labrecque, B.; de Caumia, B. Recycling of scrap tires to oil and carbon black by vacuum pyrolysis. *Resour., Conserv. Recycl.* **1990**, *51*, 203–213.

(16) Roy, C.; Chaala, A.; Darmstadt, H. The vacuum pyrolysis of used tires: End-uses for oil and carbon black products. *J. Anal. Appl. Pyrolysis* **1999**, *51*, 201–221.

(17) Benallal, B.; Roy, C.; Pakdel, H.; Chabot, S.; Porier, M. A. Characterization of pyrolytic light naphtha from vacuum pyrolysis of used tyres comparison with petroleum naphtha. *Fuel* **1995**, *74*, 1589–1594.

(18) Bridgwater, A. V.; Peacocke, G. V. C. Fast pyrolysis processes for biomass. *Renewable Sustainable Energy Rev.* **2000**, *4*, 1–73.

(19) Fortuna, F.; Cornacchia, G.; Mincarini, M.; Sharma, V. K. Pilot-scale experimental pyrolysis plant: Mechanical and operational aspects. *J. Anal. Appl. Pyrolysis* **1997**, *40*−*41*, 403–417, May 1997.

(20) Li, S. Q.; Yao, Q.; Chi, Y.; Yan, J. H.; Cen, K. F. Pilot-scale pyrolysis of scrap tires in a continuous rotary kiln reactor. *Ind. Eng. Chem. Res.* **2004**, *43*, 5133–5145.

(21) Díez, C.; Sánchez, M. E.; Haxaire, P.; Martínez, O.; Morán, A. Pyrolysis of tyres: A comparison of the results from a fixed-bed laboratory reactor and a pilot plant (rotary reactor). *J. Anal. Appl. Pyrolysis* **2005**, *74*, 254–258.

(22) San José, M. J.; Olazar, M.; Izquierdo, M. A.; Alvarez, S.; Bilbao, J. Solid trajectories and cycle-times in spouted beds. *Ind. Eng. Chem. Res.* **2004**, *43*, 3433–3438.

(23) Olazar, M.; San José, M. J.; Aguayo, A. T.; Arandes, J. M.; Bilbao, J. Design factors of conical spouted beds and jet spouted beds. *Ind. Eng. Chem. Res.* **1993**, *32*, 1245–1250.

(24) Gong, X.; Hu, G.; Li, Y. Hydrodynamic characteristics of a novel annular spouted bed with multiple air nozzles. *Ind. Eng. Chem. Res.* **2006**, *45*, 4830–4836.

(25) Olazar, M.; San José, M. J.; Zabala, G.; Bilbao, J. A new reactor in jet spouted bed regime for catalytic polymerizations. *Chem. Eng. Sci.* **1994**, *49*, 4579–4588.

(26) Olazar, M.; Arandes, J. M.; Zabala, G.; Aguayo, A. T.; Bilbao, J. Design and simulation of a catalytic polymerization reactor in dilute spouted bed regime. *Ind. Eng. Chem. Res.* **1997**, *36*, 1637–1643.

(27) Olazar, M.; Aguado, R.; Barona, A.; Bilbao, J. Pyrolysis of sawdust in a conical spouted bed reactor with a HZSM-5 catalyst. *AIChE J.* **2000**, *46*, 1025–1033.

(28) Atutxa, A.; Aguado, R.; Gayubo, A. G.; Olazar, M.; Bilbao, J. Kinetic description of catalytic pyrolysis of biomass in a conical spouted bed reactor. *Energy Fuels* **2005**, *19*, 765–774.

(29) Aguado, R.; Olazar, M.; Gaisán, B.; Prieto, R.; Bilbao, J. Kinetic study of polyolefins pyrolysis in a conical spouted bed reactor. *Ind. Eng. Chem. Res.* **2002**, *41*, 4559–4566.

(30) Aguado, R.; Olazar, M.; San José, M. J.; Gaisán, B.; Bilbao, J. Wax formation in the pyrolysis of polyolefins in a conical spouted bed reactor. *Energy Fuels* **2002**, *16*, 1429–1437.

(31) Aguado, R.; Olazar, M.; Gaisán, B.; Prieto, R.; Bilbao, J. Kinetics of polystyrene pyrolysis in a conical spouted bed reactor. *Chem. Eng. J.* **2003**, *92*, 91–99.

(32) Olazar, M.; Aguado, R.; Vélez, D.; Arabiourrutia, M.; Bilbao, J. Kinetics of scrap tyre pyrolysis in a conical spouted bed reactor. *Ind. Eng. Chem. Res.* **2005**, *44*, 3918–3924.

(33) Arabiourrutia, M.; Lopez, G.; Elordi, G.; Olazar, M.; Aguado, R.; Bilbao, J. Product distribution obtained in the pyrolysis of tyres in a conical spouted bed reactor. *Chem. Eng. Sci.* **2007**, *62*, 5271–5275.

(34) Aguado, R.; San Jose, M. J.; Olazar, M.; Alvarez, S.; Bilbao, J. Defluidization modelling during pyrolysis of plastics in a spouted bed reactor. *Chem. Eng. Process.* **2005**, *44*, 231–235.

(35) San Miguel, G.; Aguado, J.; Serrano, D. P.; Escola, D. P. Thermal and catalytic conversion of used tyre rubber and its polymeric constituents using Py-GC/MS. *Appl. Catal. B: Environ.* **2006**, *64*, 209–219.

(36) Williams, P. T.; Brindle, A. J. Catalytic pyrolysis of tyres: influence of catalyst temperature. *Fuel* **2002**, *81*, 2425–2434.

(37) Shen, B.; Wu, C.; Wang, R.; Guo, B.; Liang, C. Pyrolysis of waste tyres with zeolite USY and ZSM-5 catalysts. *Appl. Catal. B: Environ.* **2007**, *73*, 150–157.

(38) Shen, B.; Wu, C.; Wang, R.; Guo, B.; Liang, C. Pyrolysis of scrap tyres with zeolite USY. *J. Hazard. Mater.* **2006**, *137*, 1065–1073.

(39) Shen, B.; Wu, C.; Liang, C.; Guo, B.; Wang, R. Pyrolysis of waste tyres: The influence of USY catalyst/tyre ratio on products. *J. Anal. Appl. Pyrolysis* **2007**, *78*, 243–249.

(40) Williams, P. T.; Brindle, A. J. Fluidised bed catalytic pyrolysis of scrap tyres: Influence of catalyst, tyre ratio and catalyst temperature. *Waste Manag. Res.* **2002**, *20*, 546–555.

(41) Benito, P. L.; Aguayo, A. T.; Gayubo, A. G.; Bilbao, J. Catalyst equilibration for transformation of methanol into hydrocarbons by reaction-regeneration cycles. *Ind. Eng. Chem. Res.* **1996**, *35*, 2177–2182.

(42) Aguayo, A. T.; Gayubo, A. G.; Ereña, J.; Olazar, M.; Arandes, J. M.; Bilbao, J. Isotherms of chemical adsorption of bases on solid catalysts for acidity measurement. *J. Chem. Technol. Biotechnol.* **1994**, *60*, 141–146.

(43) Gayubo, A. G.; Benito, P. L.; Aguayo, A. T.; Olazar, M.; Bilbao, J. Relationship between surface acidity and activity of HZSM5 zeolite based catalysts in the transformation of methanol into hydrocarbons. *J. Chem. Technol. Biotechnol.* **1996**, *65*, 186–192.

(44) Olazar, M.; San José, M. J.; Aguayo, A. T.; Arandes, J. M.; Bilbao, J. Stable operation conditions for gas-solid contact regimes in conical spouted beds. *Ind. Eng. Chem. Res.* **1992**, *31*, 1784–1791.

(45) San José, M. J.; Olazar, M.; Aguayo, A. T.; Arandes, J. M.; Bilbao, J. Expansion of spouted beds in conical contactors. *Chem. Eng. J.* **1993**, *51*, 45–52.

(46) Olazar, M.; San José, M. J.; Alvarez, S.; Morales, A.; Bilbao, J. Design of conical spouted beds for the handling of low density solids. *Ind. Eng. Chem. Res.* **2004**, *43*, 655–661.

(47) Olazar, M.; San José, M. J.; Aguado, R.; Gaisán, B.; Bilbao, J. Bed voidage in conical sawdust beds in the transition regime between spouting and jet spouting. *Ind. Eng. Chem. Res.* **1999**, *38*, 4120–4122.

(48) San José, M. J.; Olazar, M.; Peñas, F. J.; Arandes, J. M.; Bilbao, J. Correlation for calculation of the gas dispersion coefficient in conical spouted beds. *Chem. Eng. Sci.* **1995**, *50*, 2161–2172.

(49) Williams, P. T.; Brindle, A. J. Aromatic chemicals from the catalytic pyrolysis of scrap tyres. *J. Anal. Appl. Pyrolysis* **2003**, *67*, 143–164.

(50) Arandes, J. M.; Abajo, I.; Fernández, I.; Azkoiti, M. J.; Bilbao, J. Effect of HZSM-5 zeolite addition to a FCC catalyst. Study in a laboratory reactor operating under industrial conditions. *Ind. Eng. Chem. Res.* **2000**, *39*, 1917–1924.

(51) den Hollander, M. A.; Wissink, M.; Makkee, M.; Moulijn, J. A. Gasoline conversion: reactivity towards cracking with equilibrated FCC and ZSM-5 catalysts. *Appl. Catal., A* **2002**, *223*, 85–102.

(52) den Hollander, M. A.; Wissink, M.; Makkee, M.; Moulijn, J. A. Synergy effects of ZSM-5 addition in fluid catalytic cracking of hydrotreated flashed distillate. *Appl. Catal., A* **2002**, *223*, 103–119.

(53) Williams, P. T.; Brindle, A. J. Fluidised bed pyrolysis and catalytic pyrolysis of scrap tyres. *Environ. Technol.* **2002**, *24*, 921–929.

(54) Olazar, M.; Aguado, R.; Arabiourrutia, M.; Lopez, G.; Barona, A.; Bilbao, J.; Catalyst effect on the composition of tire pyrolysis products. *Energy Fuels*. **2008**, In press.

(55) Aranda, A.; Murillo, R.; García, T.; Callén, M. S.; Mastral, A. M. Steam activation of tyre pyrolytic carbon black: Kinetic study in a thermobalance. *Chem. Eng. J.* **2007**, *126*, 79–85.

(56) Aguayo, A. T.; Benito, P. L.; Gayubo, A. G.; Olazar, M.; Bilbao, J. Acidity deterioration and coke deposition in a H-ZSM-5 zeolite in the MTG process. *Stud. Surf. Sci. Catal.* **1994**, *88*, 567–572.

(57) Guisnet, M.; Magnoux, P. Organic chemistry of coke formation. *Appl. Catal., A* **2001**, *212*, 83–96.

Received for review March 7, 2008
Revised manuscript received July 1, 2008
Accepted July 11, 2008

IE800376D